Spatial and Spectral Evolution of Solar Flares in the HXRs and Ultraviolet

Lilly Bralts-Kelly[a], Jiong Qiu[b]

a - Department of Physics and Astronomy, Macalester College
b - Department of Physics, Montana State University

ABSTRACT

Magnetic reconnection in the solar corona releases energy, heats plasmas, and generates emission in both the ultraviolet (UV) and hard X-rays (HXRs). A possible negative correlation is shown to exist between the index of an HXR photon flux spectrum and the magnetic reconnection rate measured during a solar flare. Evidence is also presented of a potential relationship between the HXR spectral index and the spatial evolution of UV flare ribbons.

BACKGROUND

Magnetic reconnection is the process by which magnetic field lines are rearranged and magnetic energy is released to heat plasmas and accelerate particles. HXR emission is produced by these particles that impact the chromosphere or the corona. UV emission is also generated when the chromosphere is heated.

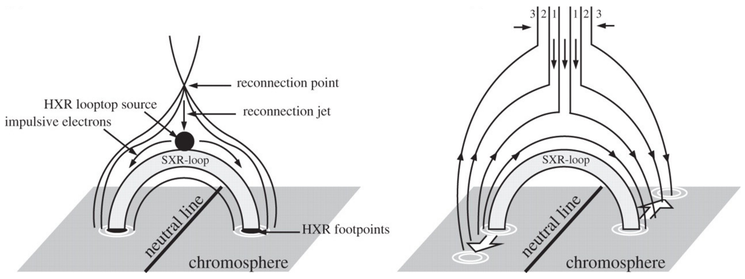

Figure 1. A visual representation of magnetic reconnection in the corona. (a) shows the locations of potential HXR sources at the time of magnetic reconnection; (b) displays the potential for ribbon elongation and spreading as reconnection occurs.

UV emission in the chromosphere is generally traced to footpoints of magnetic loops formed and heated by magnetic reconnection, whereas HXR emission may be generated at the top or at the footpoints of these loops. The location of these sources may change as the flare develops, which provides information to help us infer the progress of magnetic reconnection in the corona.

METHODS

Spatial evolution of 13 solar flares between 2011 and 2014 was mapped in the ultraviolet spectrum using data from the Solar Dynamics Observatory Atmospheric Imaging Assembly (SDO/AIA). This evolution was then classified according to the type of motion exhibited by the flare ribbons, as shown in Figure 2.

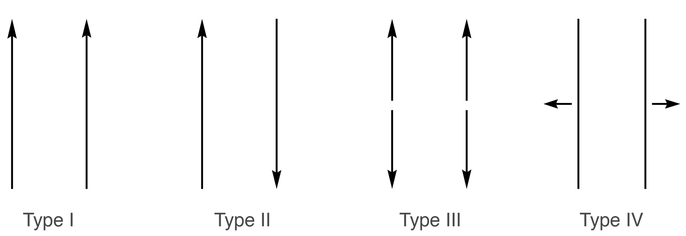

Figure 2. Classification types for solar flare ribbons in the ultraviolet. Types I, II, and III exhibit forms of parallel or antiparallel motion, while Type IV focuses on the “spreading” caused by the closing of the magnetic arcade.

The same 13 flares were then imaged in the 12-25 keV band HXR spectrum using data from the Reuven Ramaty High Energy Solar Spectroscopic Imager (RHESSI) telescope. Semi-calibrated photon spectra of HXR emission for each event were also produced, using one of the instrument’s detectors as representative of the sample.

The HXR photon spectra were fitted using a power-law function

$$F \sim F_0 \left(\frac{E}{E_0} \right)^{-\gamma}$$

where F is the photon flux, E the photon energy, and γ the photon spectral index. F_0 is the photon flux at cutoff energy E_0.

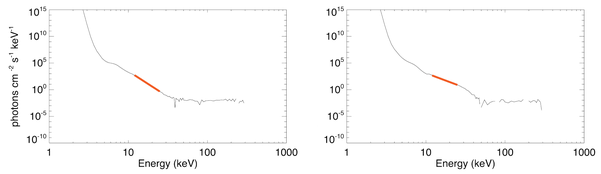

Figure 3. Plots of the semi-calibrated photon spectrum at two different times during a flare event. The 12-25 keV band fitted with a least-squares line is highlighted in orange. The slope of this line, or spectral index, provides insight into the energetic development of the flare over time.

RESULTS

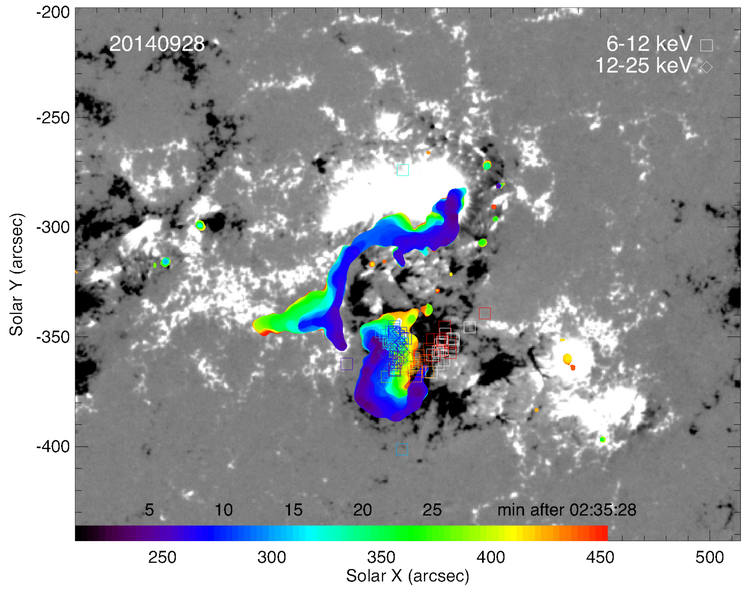

Figure 4. A solar flare event from 28 September 2014. Emission measured at 1600 Å shows the spatial evolution in time of a solar flare. Small squares show the location of the HXR centroid as time progresses. This particular event exhibits both Type III and Type IV ribbon motion.

UV maps of the 13 flares overlaid with plots of HXR source centroids were examined to compare the spatial evolution of flares in time at different wavelengths. The HXR emissions were often found to be stationary and centralized to a single looptop source, while UV Type IV motion was the most commonly observed. This suggests that magnetic reconnection moves to higher altitude, forming taller loops after the initial stage of the flare when reconnection proceeds horizontally.

Date	Type	HXR motion
2011-04-22	III, IV	Stationary, skewed
2013-08-12	II, IV	Follows ribbon elongation
2013-08-30	III, IV	Stationary, skewed
2014-02-05	III	Follows ribbon elongation
2014-05-10	III, IV	Stationary, centered
2014-06-15	III, IV	Stationary, centered
2014-09-28	III, IV	Stationary, skewed
2014-11-09	III, IV	Follows ribbon elongation
2014-12-01	I	Stationary, centered
2014-12-04	III, IV	Stationary, skewed
2014-12-17 (1)	I	Stationary, centered
2014-12-17 (2)	II, IV	Stationary, highly skewed
2014-12-19	III, IV	Stationary, centered

Figure 5. UV ribbon classifications and brief, qualitative descriptions of HXR source motion for the 13 flares analyzed. The UV ribbon types are differentiated by color to emphasize the frequency at which Types III and IV appear.

The classification of the UV motion of each flare shows that Types III and IV were the most commonly observed. Further examination of UV maps suggests a distinct point in time for each flare at which ribbon elongation (Types I, II, III) stops and Type IV motion begins. In order to more quantitatively compare data from different wavelengths, the HXR spectral index and total counts were plotted against the total reconnection rate, which is the amount of magnetic flux being reconnected per second, and UV lightcurve.

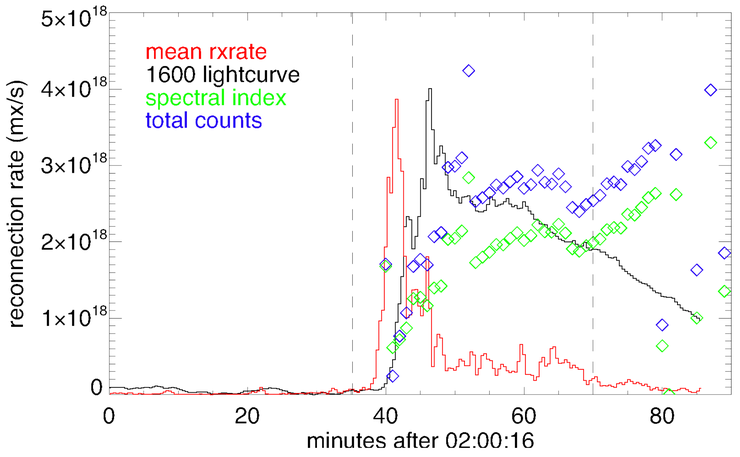

Figure 6. The spectral index and total counts (proportional to the total photon flux) overlaid on scaled plots of the mean reconnection rate and UV lightcurve for an event on 28 September 2014. The dashed vertical lines show the time interval over which the UV maps in Figure 4 were created.

These plots show consistent negative correlation between the reconnection rate and the spectral index, suggesting that increased rates of magnetic reconnection are related to lower spectral indices and therefore “harder” spectra. A tentative connection may also be drawn between the spectral index and the classification type of UV ribbon motion, although more data will be necessary to confirm any relationship.

CONCLUSIONS

— Types III and IV ribbon motion are most frequently exhibited.
— HXR spectral index and reconnection rate may be negatively correlated.
— There exists a tentative relationship between the HXR spectral index and the type of ribbon motion in the ultraviolet.

REFERENCES

Grigis, P. C. & Benz, A. O. 2008, ApJ, 683, 1180
Qiu, J., Liu, W. Hill, N. Kazachenko, M. 2010, ApJ, 725, 1
Qiu, J., Longcope, D. W., Cassak, P. A., & Priest, E. R. 2017, ApJ, 838, 1
Vilmer, N. 2012, RSPTA, 370, 1970

ACKNOWLEDGMENTS

I would like to acknowledge the funding to Dr. Jiong Qiu and the Montana State University Solar Physics REU from the National Science Foundation (Grant No. 1156011). I would also like to thank Dr. Qiu, Dr. Dana Longcope, and Dr. Eric Priest for their guidance and wisdom throughout my experience at MSU.